

Short-time Monte Carlo simulation of the majority-vote model on cubic lattices

K. P. do Nascimento

*Departamento de Matemática, Universidade Regional do Cariri,
Av. Leão Sampaio, Triângulo Juazeiro do Norte, 63010-970, Brazil and*

Departamento de Estatística e Informática, Universidade Federal Rural de Pernambuco, 52171-900, Recife – PE, Brazil

L. C. de Souza

Departamento de Física, Universidade Federal Rural de Pernambuco, 52171-900, Recife – PE, Brazil

André L. M. Vilela

*Física de Materiais, Universidade de Pernambuco, 50720-001, Recife – PE, Brazil and
Center for Polymer Studies and Department of Physics, Boston University, 02215, Boston – MA, USA*

H. Eugene Stanley

Center for Polymer Studies and Department of Physics, Boston University, Boston, MA 02215, USA

A. J. F. de Souza

Departamento de Física, Universidade Federal Rural de Pernambuco, 52171-900, Recife – PE, Brazil

(Dated: August 31, 2020)

We perform short-time Monte Carlo simulations to study the criticality of the isotropic two-state majority-vote model on cubic lattices of volume $N = L^3$, with L up to 2048. We obtain the precise location of the critical point by examining the scaling properties of a new auxiliary function Ψ . We perform finite-time scaling analysis to accurately calculate the whole set of critical exponents, including the dynamical critical exponent $z = 2.027(9)$, and the initial slip exponent $\theta = 0.1081(1)$. Our results indicate that the majority-vote model in three dimensions belongs to the same universality class of the three-dimensional Ising model.

PACS numbers: 05.20.-y, 05.50.+q, 0.5.70.Jk, 05.70.Ln

I. INTRODUCTION

The short-time Monte Carlo simulations focus on the time series analysis concerning the transitory behavior of proper physical observables of the system^{1,2}. In this work, we center our investigation for the short-time dynamics of the two-state majority-vote model for values of the parameter q nearly its critical value q_c ^{3,4}. The noise parameter q acts as a social temperature, driving the order-disorder phase transition of the system. In the vicinity of the critical point, the order parameter $M(t)$ follows the following scaling relation ansatz^{1,5,6}

$$\langle M(t) \rangle = b^{-\beta/\nu} \mathcal{M}(b^{-z}t, b^{1/\nu}\varepsilon), \quad (1)$$

where $\langle \dots \rangle$ indicates average over different realizations of the dynamics, $\varepsilon = (q/q_c - 1)$, b is a spatial scale factor, β and ν are the critical exponents associated with the order parameter and with divergence of the correlation length, respectively. Here z denotes the dynamical critical exponent, while the order parameter $M(t)$ supports the scaling relation Eq. (1) for a fully ordered initial microstate, i. e., $M(0) = 1$. Nevertheless, the scaling behavior of the order parameter is also observed for other initial configurations. For the case of an initial microstate where the order parameter is nearly zero, another independent dynamic exponent^{5,7}, the initial slip exponent θ , delineates the dynamics of the system when $M(0) \simeq 0$.

From Eq. (1), it follows that⁸

$$\langle M(t) \rangle = t^{-\beta/\nu z} \mathcal{F}(t^{1/\nu z} \varepsilon), \quad (2)$$

and precisely at the critical point, where $\varepsilon = 0$, the exponent $\beta/\nu z$ is estimated by simple regression analysis. Additionally, we use the same method to estimate q_c , considering that a straight line fits the data properly only when q is close to its critical value q_c . A strong feature of this method is to avoid issues induced by the critical slowing-down phenomena, usually present in Monte Carlo simulations. The evaluations of the short-time analysis are carried out in the early stages of the dynamics, thus evading the relaxation period for the system to reach equilibrium.

Although its apparent simplicity, the above-sketched method has been successfully applied to a variety of condensed matter systems^{9–17}. For instance, the dimensional crossover for an Iron-Vanadium magnetic superlattice model observed when the inter- to intralayer exchange coupling ratio approaches zero¹⁶. The function of the iron vacancy in the magnetic order of a $J_1 - J_2$ Ising model¹⁸ is a deeply non-trivial application of the short-time method. In a lattice-gauge theory application¹⁹, the static and dynamical critical exponents of a $(2 + 1)$ -dimensional gluodynamics of the $SU(2)$ gauge theory were obtained, where the universality hypothesis was verified. Recently other applications and new developments of the short-time analysis method were also

employed⁸.

In this work, we apply a novel technique that allows the systematic and accurate evaluation of the critical point q_c , obtained from the analysis of the Monte Carlo simulations data². Furthermore, the method provides estimates for all static and dynamical critical exponents. We illustrate our method in the study of the critical behavior of the majority-vote (MV) model with noise on cubic lattices^{3,4}.

The critical behavior of the majority-vote model has been investigated by several techniques on two dimensions for distinct lattice structures^{20–22}. We also remark a number of studies and generalizations of the majority-vote dynamics which shed light on our comprehension of the non-equilibrium statistical mechanics^{23–37}.

In the standard two-state majority-vote model^{3,4}, the opinion dynamics follows the majority rule, and the opinion of an individual is represented by a spin variable σ , which assumes two values: ± 1 . A given spin adopts the state in which most of its interacting neighbors are with probability $1 - q$, and the opposite state with probability q . This system undergoes an order-disorder phase transition at a finite value of the noise parameter q , which belongs to the universality class of corresponding equilibrium Ising models in two^{3,4,20,38–40}, and probably also in three⁴¹ dimensions. These findings support the conjecture⁴² that non-equilibrium model systems with up-down symmetry and spin-flip dynamics are in the same universality class of the equilibrium Ising model.

Motivated by the results of the recent studies⁴¹, obtained from long-time Monte Carlo simulations of moderately small lattices, we decide to investigate the MV model in three-dimensions. On account of finite-size effects, the authors consider corrections terms for scaling in their analysis. On the other hand, previous results³⁹ suggested that the MV model in three dimensions could violate the conjecture we mention before. We believe it is essential to support the findings of reference⁴¹ with simulations on larger lattices, avoiding correction to the scaling, and with different strategies. We also provide the first estimates for both the dynamical critical and the initial slip exponents to this model in three dimensions.

We describe the short-time Monte Carlo data analysis in section II along with the MV model description. In the same section, we point our observations concerning the computational procedure and numerical techniques. In section III we present our results. We conclude with a summary and final remarks in section IV.

II. MODEL, THEORY AND SIMULATION

To each node of a fully periodic cubic lattice of side L , we associate a Ising-like spin variable $\sigma_i = \pm 1$. Such spin interacts with its six nearest neighbors. As a result of this interaction, the spin changes its state according to the majority rule³. During an elementary time step,

a node i is randomly selected and the spin σ_i is flipped with a probability given by

$$w(\sigma_i) = \frac{1}{2} \left[1 - (1 - 2q)\sigma_i \mathcal{S} \left(\sum_{\delta=1}^6 \sigma_{i+\delta} \right) \right], \quad (3)$$

where $\mathcal{S}(x) = \text{sgn}(x)$ if $x \neq 0$ and $\mathcal{S}(0) = 0$. The sum runs over the nearest neighbors of the spin σ_i . We measure time in Monte Carlo steps (MCS), which consists of $L \times L \times L$ such elementary moves.

In a short-time critical dynamic analysis, one prepares the system in an initial state. Then the system is released to evolve according to the prescribed dynamics for some value of the control parameter q until a specific time. The whole process is repeated a certain number of times in order to obtain a smooth averaged time series. To our purpose, it is convenient to start from a fully ordered initial state and to follow the temporal behavior of the order parameter. Therefore, at $t = 0$, we set $\sigma_i = 1$ for all $i \in N$, where $N = L^3$. Thus, the magnetization

$$M(t) = \frac{1}{L^3} \sum_i \sigma_i, \quad (4)$$

at $t = 0$ is unity.

For the ordered phase, where $q < q_c$, the system evolves toward a steady state, and $\langle M(t, q) \rangle$ decays to a constant roughly independent of the system size. On the contrary, for $q > q_c$ one expects $\langle M(t, q) \rangle$ to drop to a value of the order of $1/L$. The relaxation is exponential for q not too close to q_c ³⁵, and it turns into a power-law when q approaches q_c , c.f., Eq. (2). The overall behavior shows up more clearly when plotted in a double logarithmic scale, and it is enhanced through the following auxiliary function²

$$\Psi(t, q) = \frac{\partial}{\partial \tau} \ln \langle M(t, q) \rangle, \quad (5)$$

where $\tau = \ln(t)$. From Eq. (2), we have

$$\Psi(t, q) = -\frac{\beta}{\nu z} + t^{1/\nu z} \varepsilon \tilde{\Psi}(t^{1/\nu z} \varepsilon), \quad (6)$$

with $\tilde{\Psi}(x)$ being an universal scaling function.

Thus $\Psi(t, q)$ either goes to zero or tends to $-\infty$ with the increasing of t for $\varepsilon < 0$ or $\varepsilon > 0$, respectively. On the other hand, at the critical point $\Psi(t, q = q_c) = -\beta/\nu z$, a constant independent of t in the scaling regime. Furthermore, the family of curves $\Psi(t_i, q)$, taken at distinct times t_i , plotted against q cross at the single point $(\beta/\nu z, q_c)$. Having an estimate of the critical noise q_c , the exponent $1/\nu z$ can be obtained by plotting the curves $\Psi(t_i, q)$ against the proper scaling variable $x = t^{1/\nu z} \varepsilon$. Once all curves should collapse onto a single curve only for the correct value of this exponent when calculating x . A similar scaling plot holds to the magnetization data. According to Eq. (2), the plot of $t^{\beta/\nu z} \langle M(t, q) \rangle$ against $x = t^{1/\nu z} \varepsilon$

also collapses onto a single curve for precise values of the critical parameters. Besides that, we can explore the time evolution of the logarithmic derivative of the magnetization with respect to ε . The finite-time scaling law for the magnetization, Eq. (2), gives

$$\partial_\varepsilon \ln M(t, \varepsilon)|_{\varepsilon=0} \sim t^{1/\nu z}. \quad (7)$$

Until now, we neglected any finite-size effects. Right at the beginning of the time evolution the fluctuations are spatially uncorrelated. Thereby, the effective correlation length $\xi(t)$ is very small for small t . As t increases, $\xi(t)$ eventually becomes similar to the equilibrium correlation length $\xi_{\text{eq}}(q)$. From there on, the behavior of $\langle M(t, q) \rangle$ crosses over towards its steady-state value, which is finite for finite L , even for q above q_c . In this way, $\Psi(t, q)$ goes to zero as $t \rightarrow \infty$ independently of q . The inflection points in the $\Psi(t, q)$ curves are hallmarks of the crossover to equilibrium and a clear signal of finite-size effects. The analysis must be carried out within a time window in which $\Psi(t, q)$ presents a monotonous behavior with respect to t .

Besides the magnetization, we measure its second moment

$$M^{(2)}(t, q) = \frac{1}{L^3} \left\langle \left(\sum_i \sigma_i \right)^2 \right\rangle. \quad (8)$$

That allows for calculating the fluctuation of the order parameter

$$\Delta M(t) = \frac{1}{L^3} \left\langle \left(\sum_i \sigma_i \right)^2 \right\rangle - \frac{1}{L^3} \left\langle \sum_i \sigma_i \right\rangle^2, \quad (9)$$

and the second-order cumulant^{1,8}

$$U_2(t) = \frac{M^{(2)}}{\langle M \rangle^2} - 1. \quad (10)$$

Let us now focus on the time evolution of the magnetization starting from a disordered state. The initial microstate has magnetization $m_0 \ll 1$ and negligible spatial correlation. With this kind of initial condition, the time evolution of the magnetization at the critical noise becomes⁸ $M(t) \propto t^\theta$, where the exponent θ controls the rate of growth of the magnetization for short times. This power-law initial increase is observed only in the limit $m_0 \rightarrow 0$. In practice, data must be extrapolated for $m_0 = 0$.

In our numerical simulations, we use the parallel computing platform CUDA⁴³, developed by NVIDIA corporation. Although we do not present the implementation details, quite relevant information can be found in the reference by Preis and co-workers⁴⁴. Here we present only a brief description of our procedure.

The CUDA programming model allows us to perform simulations in a massively parallel way. We obtain data

on several cubic lattices in a single run on a Graphics Processing Unit (GPU). We increase the parallelism even further storing one spin in a single bit, i. e., 32 spins per computer word^{45,46}.

To maximize parallelization, we stack several lattices on top of each other and update them simultaneously. To avoid neighbor spins to be changed at the same time, we divide the lattice into 8 sub-lattices, and perform a Monte Carlo step in 8 iterations. In each iteration, all spins belonging to the same sub-lattice are updated in parallel. This procedure is not equivalent to randomly select one spin to flip at a time. Nevertheless, it affects only non-universal quantities, as the value of the phase transition point⁴⁷.

III. CRITICAL RELAXATION OF THE THREE-DIMENSIONAL MAJORITY VOTE MODEL

We perform Monte Carlo simulations on three-dimensional lattices of linear sizes $L = 256, 512, 1024$, and 2048, with periodic boundary conditions. We focus our presentation for different initial conditions: (a) for $L = 256$ with a fully ordered initial state, and (b) for $L = 2048$ with a disordered initial configuration, where $m_0 \simeq 0$.

A. Ordered initial state

We investigate the time behavior for a variety of physical quantities defined on a cubic lattice with periodic boundary conditions and side $L = 256$. We choose a fully ordered initial state, and we record the magnetization up to 10^4 MCS for several values of the noise q near q_c . In each simulation, we generate 1024 independent samples for a given noise value q . We reproduce the simulations using the same noise until we obtain data smooth enough to calculate reliable numerical derivatives.

In Fig. 1, we show the time evolution of the magnetization averaged over at least 5120 samples. We report the representative results, although we carried out simulations for many noises in the range of $0.17722 \leq q \leq 0.17737$. For the sake of clarity, we do not display the error bars. For noises values below the critical point, the magnetization relaxes from the initial non-equilibrium state toward a finite amount. This behavior indicates the presence of long-range order. Above the critical noise, the curves lean down, signaling that the system is in a disordered phase. At the critical noise, the magnetization develops a slow power-law decay after a microscopic transient time.

In Fig. 2, we show the auxiliary function $\Psi(t, q)$ as a function of $\ln(t)$ for the same noises as in Fig. 1. Now, one sees a clearer signature of the critical point. For noises values below the critical one, the auxiliary function goes to zero in the long-time regime due to the residual

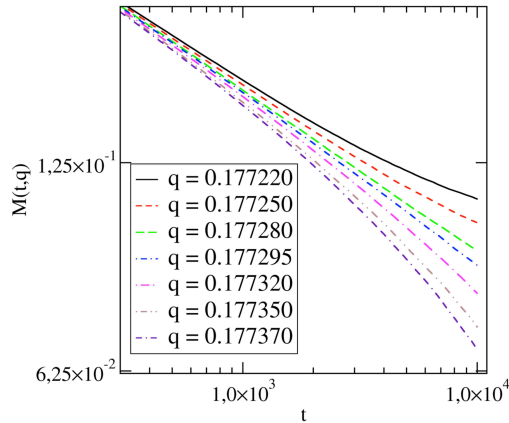


FIG. 1. (Color online) Average magnetization as a function of time for $L = 256$ and several values of the noise near the critical point $q_c = 0.177293$. Below the critical noise, it shows a trend to saturate in the long-time regime, indicating the presence of an ordered steady-state. The average magnetization displays a faster than power-law decay above the critical noise.

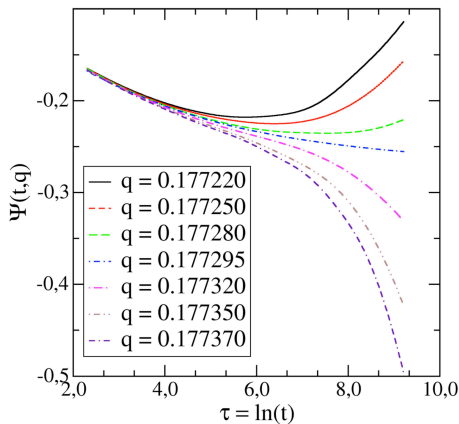


FIG. 2. (Color online) The auxiliary function $\Psi(t, q)$ as a function of $\ln(t)$ in the vicinity of the critical point $q_c = 0.177293$.

ordering of the system. On the other hand, $\Psi(t, q)$ assumes diverging negative values above the critical point, reflecting the exponential relaxation towards the disordered steady-state. Precisely at the critical point, it assumes a constant value after a microscopic transient time. From the data of Fig. 2, it is possible infer that the critical noise is close to $q = 0.17729$.

As stated before, we can obtain a more precise estimate of the critical point location by plotting the data of Fig. 2 in a different form, specifically, considering $\Psi(t, q)$ as a

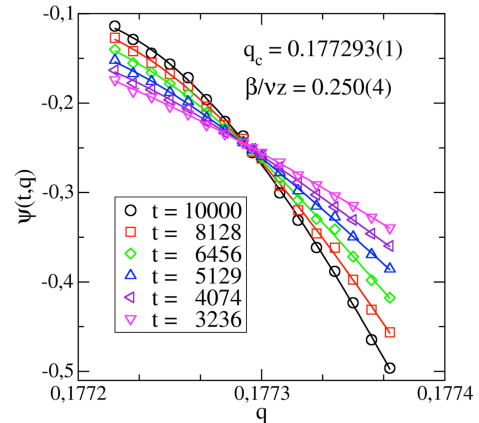


FIG. 3. (Color online) The auxiliary function $\Psi(t, q)$ versus q taken at distinct times. All curves intersect at a single point, identifying the critical noise q_c and the exponent ratio $\beta/\nu z$. We estimate $q_c = 0.177293(1)$ and $\beta/\nu z = 0.250(4)$.

function of q for a selected set of values of t . In Fig. 3, we plot the auxiliary function $\Psi(t, q)$, as a function of the noise q , for a selected set of run times. The curves have a common intersection point $(q_c, -\beta/\nu z)$, in which the auxiliary function does not depend on time t . All curves cross at virtually one single point. The notably narrow spread of the crossings is a definite indication that no relevant corrections to scaling are present in the data. From these crossings, we estimate $q_c = 0.177293(1)$ and $\beta/\nu z = 0.250(4)$. We compare our estimate for q_c with $q_c = 0.17628(7)$ from reference⁴¹. The disagreement between the two estimates is due to the different updating schemes employed in each simulation.

Owning an accurate estimate of the critical noise, we can determine the dynamic critical exponent z , from the temporal evolution of the second-order cumulant defined by Eq. (10). To obtain a direct estimative for z , we perform simulations at the critical noise $q_c = 0.177293$ on lattices of side $L = 256$, for 10240 independent samples. According to the finite-time scaling behavior, the second cumulant shall grow in time as $U_c(t) \propto t^{d/z}$ at the critical point, where d is the space dimension⁸. In the upper panel of Fig. 4, we present our data for $U_2(t)$ at the critical noise q_c . From these data we got $3/z = 1.480(7)$. Besides the exponent z , the new data provide an estimate of $\beta/\nu z$ more accurate than that obtained from the intersections of the curves in Fig. 3, owing to its superior statistical quality. In the bottom panel of Fig. 4, we report the time evolution of the magnetization at the critical point, from which we accurately estimate $\beta/\nu z = 0.2567(9)$.

To obtain an estimate of the $1/\nu z$, we notice from Fig. 5 that the magnetization as a function of noise at a given time is fairly linear. Hence, the data corresponding to, say, $t = t_i$ is well described by $M(t_i, q) =$

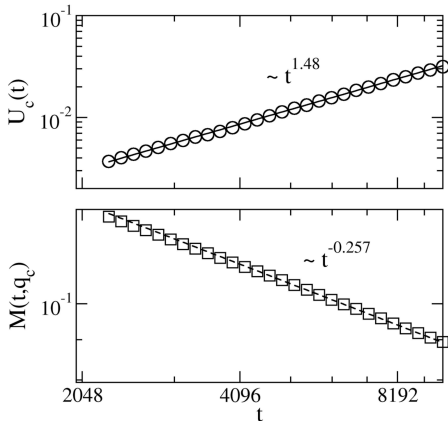


FIG. 4. (Color online) (Top) Time-evolution of the second cumulant $U_2(t)$ calculated at the critical noise. Continuous line corresponds to the power-law growth $U(t) \propto t^{3/z}$. (Bottom) Time-evolution of the magnetization at the critical noise. The dashed line is consistent with the power-law decaying $M(t) \propto t^{-\beta/\nu z}$.

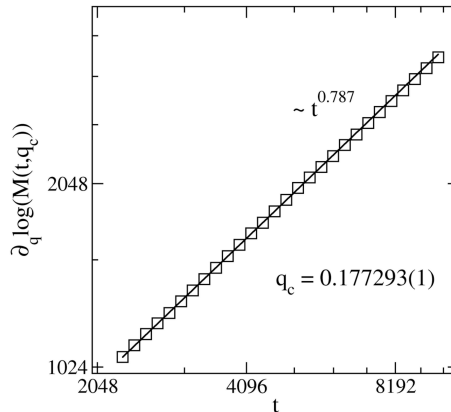


FIG. 6. (Color online) Time evolution of the logarithmic derivative of the magnetization at the critical noise $q_c = 0.177293(1)$. Continuous line corresponds to the power-law growth $\partial_q \log M(t) \propto t^{1/\nu z}$.

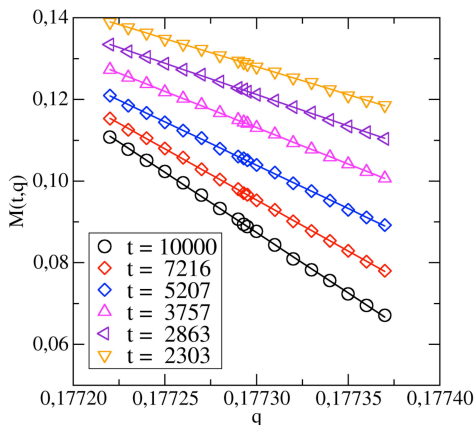


FIG. 5. (Color online) Magnetization as a function of q for several values of t . The results are well fitted by straight lines. The error bars are smaller than the symbol sizes.

$c_{0,i} + qc_{1,i}$, where $c_{0,i}$ and $c_{1,i}$ are calculated by a least-square method. Thus

$$\partial_q \log M(t, q)|_{t=t_i} = \frac{c_{1,i}}{c_{0,i} + qc_{1,i}}, \quad (11)$$

for any q in the range $[0.17722, 0.17737]$.

In Fig. 6, we exhibit the time evolution of the logarithmic derivative of the magnetization with respect to q at the critical noise. The slope of the straight line provides $1/\nu z = 0.7869(16)$.

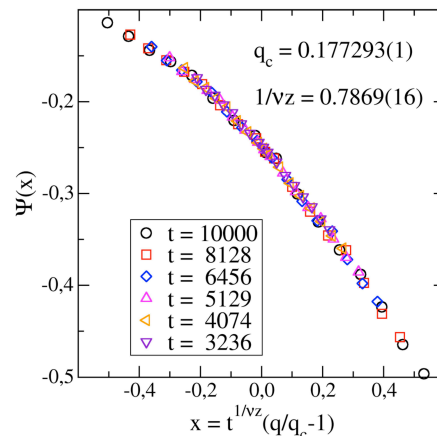


FIG. 7. (Color online) The auxiliary function data plotted against the scaling variable $x = t^{1/\nu z}(q/q_c - 1)$.

According to the finite-time scaling hypothesis the data from both Fig. 3 and Fig. 5 should collapse onto a single curve, provided that their respective axes be properly rescaled. This scaling analysis can be used to further verify the precision of the above estimates for the critical parameter of the three-dimensional MV model. In Fig. 7, we plot our data for the auxiliary function $\Psi(t, q)$ as a function of $x = t^{1/\nu z}(q/q_c - 1)$. Similarly, we plot $t^{\beta/\nu z}M(t, q)$ against x in Fig 8. The plots of Fig. 7 and Fig 8 show excellent agreement with the finite-time scaling assumption. They also give evidence of the correctness of our estimates for the critical parameters.

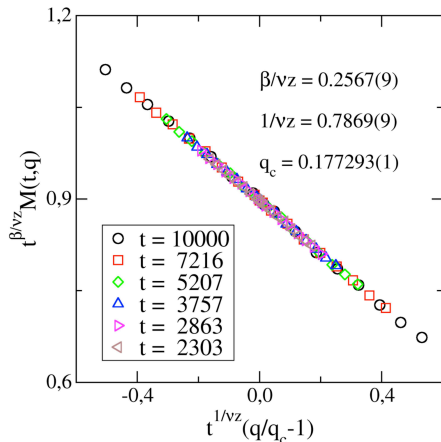


FIG. 8. (Color online) Data collapse of the magnetization data computed at distinct times and noises. The data collapse validates our estimates for the critical parameters $\beta/\nu z$, $1/\nu z$, and q_c .

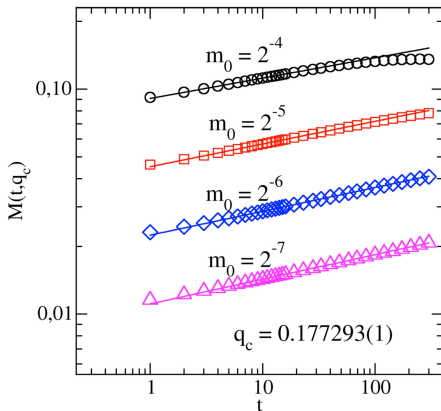


FIG. 9. (Color online) Time evolution of the averaged magnetization at the critical noise $q_c = 0.177293(1)$ starting from disordered microstates. Lines correspond to the power-law growth $M(t) \propto t^\theta$. This result provides $\theta = 0.1081(1)$.

B. Disordered initial state

To estimate the initial slip exponent, we simulate the short-time evolution of the magnetization in cubic lattices of side $L = 2048$ for 300 MCS, starting from a disordered initial state. We measure the magnetization $M(t)$ for $m_0 = 2^{-4}, 2^{-5}, 2^{-6}, 2^{-7}$, and 2^{-8} . For each case, we average $M(t)$ over 16 initial conditions and time history. We summarize our results in Fig. 9, where we display the time evolution of magnetization for several values of m_0 . As shown in Table I, the measured exponent θ depends

on the initial magnetization m_0 . From these data, we apply the BulirschStoer (BST) extrapolation method⁴⁸ to obtain $\theta = 0.1081(1)$ for $m_0 = 0$. We remark that models belonging to distinct stationary universality class can present the same dynamic initial slip exponent⁴⁹.

IV. CONCLUSIONS

We have investigated the majority-vote model in three-dimensional cubic lattices using large-scale GPU Monte Carlo simulations. We accurately followed the short-time critical relaxation process from both fully ordered and disordered initial states. In our analysis, we use regular cubic lattices large enough for finite-size effects to be negligible during the simulation. Besides, we were able to investigate the deep scaling regime for a time interval that is sufficiently long to eliminate the need corrections to the scaling. We obtain the critical parameters of the system by exploring the scaling properties of a new auxiliary function defined by Eq. (5) along with the order parameter. This function provides a precise location of the critical point of the system. Thus, we obtain the critical noise $q_c = 0.177293(1)$, associated with the critical exponent ratios $\beta/\nu z = 0.2567(9)$, and $1/\nu z = 0.7869(16)$. In addition, we calculate the dynamical critical exponent $z = 2.027(9)$ by the time evolution of the second-order cumulant, and the initial slip exponent $\theta = 0.1081(1)$ by the initial increase of the magnetization (starting from a disordered state). From this set of exponents our results provide the following estimates of the static critical exponents $\beta = 0.3262(13)$ and $\nu = 0.627(4)$. These values are in complete agreement with the three-dimensional Ising universality class. Recent large-scale Monte Carlo study of a 3D Ising model yields $\nu = 0.629912(86)$ ⁵⁰. Estimates based on field-theoretical methods provide $\beta = 0.32645(6)$ and $\nu = 0.62999(5)$ ⁵¹. Our results also agree with the long-time Monte Carlo simulations of the MV model, where $\beta = 0.331(34)$ and $\nu = 0.626(11)$ ⁴¹. We believe this is the first work to obtain the dynamic critical exponents θ and z for the majority-vote model in three-dimensional regular lattices. Nevertheless, our findings are very close to $z = 2.03(4)$ ⁵², $z = 2.0245(15)$ ⁵³, and $\theta = 0.108(2)$ ⁵⁴ from simulations of the three-dimensional Ising model. Therefore, the majority-vote model in three-dimensions belongs to the three-dimensional Ising universality class.

We remark that the method of analyzing data from short-time critical dynamics using the auxiliary function Ψ is quite general, and adequately robust to investigate the critical behavior of further complex statistical systems.

ACKNOWLEDGMENTS

To the bright memory of our wonderful and dedicated friend and teacher F. G. Brady Moreira, who recently

TABLE I. Critical parameters for the majority-vote and Ising models in three dimensions.

m_0	0.00390625	0.0078125	0.015625	0.03125	0.0625
θ	0.1082(3)	0.1074(2)	0.10578(4)	0.10086(9)	0.0904(1)

passed away.

The authors acknowledge financial support from NVIDIA Data Science GPU Program, and the fund-

ing agencies FACEPE (APQ-0565-1.05/14, APQ-0707-1.05/14), CAPES, and CNPq. The Boston University work was supported by NSF Grant PHY-1505000.

-
- ¹ B. Zheng, International Journal of Modern Physics B **12**, 1419 (1998).
- ² L. C. de Souza, A. J. F. de Souza, and M. L. Lyra, Phys. Rev. E **99**, 052104 (2019).
- ³ M. J. de Oliveira, Journal of Statistical Physics **66**, 273 (1992).
- ⁴ M. J. de Oliveira, J. F. F. Mendes, and M. A. Santos, Journal of Physics A: Mathematical and General **26**, 2317 (1993).
- ⁵ H. K. Janssen, B. Schaub, and B. Schmittmann, Zeitschrift für Physik B Condensed Matter **73**, 539 (1989).
- ⁶ Z. Li, U. Ritschel, and B. Zheng, Journal of Physics A: Mathematical and General **27**, L837 (1994).
- ⁷ D. A. Huse, Phys. Rev. B **40**, 304 (1989).
- ⁸ E. V. Albano, M. A. Bab, G. Baglietto, R. A. Borzi, T. S. Grigera, E. S. Loscar, D. E. Rodriguez, M. L. R. Puzzo, and G. P. Saracco, Reports on Progress in Physics **74**, 026501 (2011).
- ⁹ H. J. Luo, M. Schulz, L. Schülke, S. Trimper, and B. Zheng, Physics Letters A **250**, 383 (1998).
- ¹⁰ L. F. da Silva, U. L. Fulco, and F. D. Nobre, J. Phys.: Condens. Matter **21**, 346005 (2009).
- ¹¹ S. Yin, P. Mai, and F. Zhong, Phys. Rev. B **89**, 144115 (2014).
- ¹² M. Santos, Phys. Rev. E **61**, 7204 (2000).
- ¹³ M. Zelli, K. Boese, and B. W. Southern, Phys. Rev. B **76**, 224407 (2007).
- ¹⁴ R. da Silva, N. A. Alves, and J. R. Drugowich de Felicio, Phys. Rev. E **66**, 026130 (2002).
- ¹⁵ J. Q. Yin, B. Zheng, and S. Trimper, Phys. Rev. E **72**, 036122 (2005).
- ¹⁶ A. K. Murtazaev and V. A. Mutailamov, Journal of Experimental and Theoretical Physics **116**, 604 (2013).
- ¹⁷ A. Brunstein and T. Tomé, Phys. Rev. E **60**, 3666 (1999).
- ¹⁸ N. J. Zhou, B. Zheng, and J. H. Dai, Phys. Rev. E **87**, 022113 (2013).
- ¹⁹ R. B. Frigori, Computer Physics Communications **181**, 1388 (2010).
- ²⁰ M. A. Santos and S. Teixeira, Journal of statistical physics **78**, 963 (1995).
- ²¹ P. R. A. Campos, V. M. de Oliveira, and F. G. B. Moreira, Phys. Rev. E **67**, 026104 (2003).
- ²² A. L. Acuña-Lara, F. Sastre, and J. R. Vargas-Arriola, Phys. Rev. E **89**, 052109 (2014).
- ²³ T. Tomé and M. J. de Oliveira, Physical Review E **58**, 4242 (1998).
- ²⁴ A. L. M. Vilela, F. G. B. Moreira, and A. J. F. de Souza, Physica A: Statistical Mechanics and its Applications **391**, 6456 (2012).
- ²⁵ A. L. M. Vilela, B. J. Zubillaga, C. Wang, M. Wang, R. Du, and H. E. Stanley, Scientific Reports **10**, 8255 (2020).
- ²⁶ A. L. M. Vilela and A. J. F. de Souza, Physica A **488**, 216 (2017).
- ²⁷ M. M. de Oliveira, M. G. E. da Luz, and C. E. Fiore, Physics Review E **97**, 060101 (2018).
- ²⁸ A. R. Vieira and N. Crokidakis, Physica A: Statistical Mechanics and its Applications **450**, 30 (2016).
- ²⁹ L. Crochik and T. Tomé, Physical Review E **72**, 057103 (2005).
- ³⁰ T. E. Stone and S. R. McKay, Physica A: Statistical Mechanics and its Applications **419**, 437 (2015).
- ³¹ A. L. M. Vilela and F. G. B. Moreira, Physica A: Statistical Mechanics and its Applications **388**, 4171 (2009).
- ³² D. Stauffer and K. Kulakowski, Journal of Statistical Mechanics: Theory and Experiment **2008**, P04021 (2008).
- ³³ J.-M. Drouffe and C. Godrche, Journal of Physics A: Mathematical and General **32**, 249 (1999).
- ³⁴ B. Derrida, J. L. Lebowitz, E. R. Speer, and H. Spohn, Journal of Physics A: Mathematical and General **24**, 4805 (1991).
- ³⁵ L. S. A. Costa and A. J. F. de Souza, Physical Review E **71**, 056124 (2005).
- ³⁶ F. W. S. Lima, International Journal of Modern Physics C **26**, 1550035 (2015).
- ³⁷ L. F. C. Pereira and F. G. B. Moreira, Phys. Rev. E **71**, 016123 (2005); See also: C. I. N. Sampaio-Filho and F. G. B. Moreira, *ibid.* **88**, 032142 (2013).
- ³⁸ J. F. F. Mendes and M. A. Santos, Phys. Rev. E **57**, 108 (1998).
- ³⁹ J. S. Yang, I. M. Kim, and W. Kwak, Physical Review E **77**, 051122 (2008).
- ⁴⁰ G. Ódor, Rev. Mod. Phys. **76**, 663 (2004).
- ⁴¹ A. L. Acuña-Lara and F. Sastre, Phys. Rev. E **86**, 041123 (2012).
- ⁴² G. Grinstein, C. Jayaprakash, and Y. He, Phys. Rev. Lett. **55**, 2527 (1985).
- ⁴³ NVIDIA Corporation, *NVIDIA CUDA Compute Unified Device Architecture Programming Guide* (NVIDIA Corporation, 2015).
- ⁴⁴ T. Preis, P. Virnau, W. Paul, and J. J. Schneider, Journal of Computational Physics **228**, 4468 (2009).
- ⁴⁵ P. M. C. Oliveira, *Computing Boolean Statistical Models* (World Scientific, 1991).
- ⁴⁶ A. J. F. de Souza and F. G. B. Moreira, Phys. Rev. B **48**, 9586 (1993).
- ⁴⁷ N. Menyhárd and G. Ódor, Brazilian Journal of Physics **30**, 113 (2000).
- ⁴⁸ N. A. Alves, J. R. D. de Felicio, and U. H. E. Hansmann,

- Journal of Physics A: Mathematical and General **33**, 7489 (2000).
- ⁴⁹ V. Volpati, U. Basu, S. Caracciolo, and A. Gambassi, Phys. Rev. E **96**, 052136 (2017).
- ⁵⁰ A. M. Ferrenberg, J. Xu, and D. P. Landau, Phys. Rev. E **97**, 043301 (2018).
- ⁵¹ P. Lundow and I. Campbell, Physica A: Statistical Mechanics and its Applications **511**, 40 (2018).
- ⁵² S. Wansleben and D. P. Landau, Phys. Rev. B **43**, 6006 (1991).
- ⁵³ M. Hasenbusch, Phys. Rev. E **101**, 022126 (2020).
- ⁵⁴ A. Jaster, J. Mainville, L. Schlke, and B. Zheng, Journal of Physics A: Mathematical and General **32**, 1395 (1999).